QCD corrections to Higgs boson production and $H \to b\bar{b}$ decay in weak boson fusion

Konstantin Asteriadis,[1,*] Arnd Behring,[2,†] Kirill Melnikov,[3,‡] Ivan Novikov,[3,§] and Raoul Röntsch[4,‖]

[1]*Institute for Theoretical Physics, University of Regensburg, 93040 Regensburg, Germany*
[2]*Theoretical Physics Department, CERN, 1211 Geneva 23, Switzerland*
[3]*Institute for Theoretical Particle Physics, Karlsruhe Institute of Technology, 76128 Karlsruhe, Germany*
[4]*Tif Lab, Dipartimento di Fisica, Università di Milano and INFN, Sezione di Milano, Via Celoria 16, I-20133 Milano, Italy*

(Received 18 July 2024; accepted 12 August 2024; published 16 September 2024)

We study QCD corrections to the process where a Higgs boson is produced in weak boson fusion and then decays into a pair of massive b quarks. We find that typical experimental criteria used to identify b jets in this process affect QCD corrections to the decay, making it necessary to account for them in the proper description of this process. Indeed, if corrections to the production and decay are combined, the fiducial cross section of the weak boson fusion process $pp \to H(\to b\bar{b})jj$ is reduced by about 40% relative to leading-order predictions, compared to just about 8% if only corrections to the production process are considered. We investigate the origin of these large corrections through next-to-next-to-leading order and conclude that they appear because a number of independent moderately large effects conspire to significantly reduce the fiducial cross section for this process.

DOI: 10.1103/PhysRevD.110.054017

I. INTRODUCTION

Detailed studies of the Higgs boson will continue to play a central role in the physics program of the Large Hadron Collider during Run 3 and the high-luminosity phase. They are expected to expand, refine, and consolidate the many important results in Higgs boson physics obtained since the Higgs boson discovery, which have given us a good understanding of the different properties of this particle and confirmed its central role in breaking electroweak symmetry. With more data, improved detection capabilities, and novel analysis strategies, established Higgs boson signatures will be studied with greater precision, and rare signals may become accessible for the very first time.

Profiling the Higgs boson necessitates measurements of its couplings to matter and gauge fields, as well as its quantum numbers [1,2]. Of the couplings, the Yukawa interactions are currently among the least known, and there is huge interest in learning more about them. Indeed, currently, there is no information about the Yukawa couplings of fermions of the first generation, while those of the third-generation fermions have been measured to about 20% precision [1,2]. Because $H \to b\bar{b}$ is the dominant decay mode of the Higgs boson, one would think that it should be straightforward to measure it and hence determine the bottom quark Yukawa coupling y_b. However, reaching the current precision has proven to be a challenging endeavor. The principal reason for this is that it is difficult to identify b jets from Higgs boson decays over the much more numerous b jets arising from quantum chromodynamics (QCD) backgrounds. It was pointed out in Ref. [3] that requiring a boosted Higgs boson to be produced in association with either a weak vector boson or a jet could allow the $H \to b\bar{b}$ decay to be identified and studied using jet substructure techniques. Following this strategy, both the ATLAS and CMS experiments observed the $H \to b\bar{b}$ decay in associated VH production [4–7] and measured the bottom quark Yukawa coupling.

Another promising production mode which could lead to complementary studies of the $H \to b\bar{b}$ decay is weak boson fusion (WBF), $pp \to H(\to b\bar{b})jj$. In weak boson fusion, Higgs bosons are produced at central rapidities, together with two nearly back-to-back forward jets with little hadronic activity between them. This means that Higgs boson production in WBF followed by $H \to b\bar{b}$ decay can be distinguished from the QCD background by the presence of two central b jets and two forward jets, typically originating from light quarks. Indeed, in the case of WBF with $H \to b\bar{b}$ decay, ATLAS and CMS report signal strengths consistent with the Standard Model and claim

*Contact author: konstantin.asteriadis@ur.de
†Contact author: arnd.behring@cern.ch
‡Contact author: kirill.melnikov@kit.edu
§Contact author: ivan.novikov@kit.edu
‖Contact author: raoul.rontsch@unimi.it

that observed rates are about 2.5 standard deviations away from the background-only hypothesis [8–11]. These measurements will be further improved during Run 3 and beyond.

In order to distinguish the signal process from the backgrounds and to extract interesting quantities from the signal measurement, it is imperative to have the best possible theoretical predictions for both. In this paper, we focus on the next-to-leading-order (NLO) and next-to-next-to-leading-order (NNLO) QCD corrections to the signal process $pp \to H(\to b\bar{b})jj$. In the narrow width approximation, this process consists of on-shell Higgs boson production in weak boson fusion followed by the decay of the Higgs boson $H \to b\bar{b} + X$. Since the Higgs boson is a spin-zero particle, there are no spin correlations, and the factorization between production and decay would be complete if not for selection criteria applied to QCD jets from both subprocesses.

Higgs boson production in WBF has been known through NNLO accuracy in QCD at a fully differential level for about a decade [12,13].[1] Furthermore, the WBF cross sections that are inclusive with respect to QCD radiation have been computed with an astonishing N^{3}LO QCD accuracy [16]. These theoretical results allow us to reduce the uncertainties in perturbative QCD predictions for fiducial cross sections of Higgs boson production in WBF to just a few percent. Given this level of precision, one needs to critically examine other parametrically suppressed contributions which were neglected earlier, but may become relevant at the achieved level of precision. Such effects include electroweak corrections to Higgs boson production in WBF [17,18], interference effects in collisions of identical quarks [17,18], as well as non-factorizable contributions that describe a crosstalk between the two incoming quark legs and appear for the first time at NNLO in QCD [19–23]. The results of these analyses lead to the conclusion that the effects mentioned above provide percent-level corrections to WBF fiducial cross sections, which should be included in the most up-to-date theoretical predictions for this quantity.

Interestingly, in spite of this enormous effort, the impact of Higgs boson decays on the magnitude of radiative corrections in weak boson fusion remained largely unexplored. Understanding this is particularly important for the $H \to b\bar{b}$ decay channel because of the rich jet environment in this process and the selection criteria used to identify it. While the WBF-production jets and the decay jets typically populate different regions of phase space, identifying b jets requires them to pass a certain $p_\perp$ threshold. This selects events with particular values of the Higgs boson transverse momentum and impacts the magnitude of radiative corrections [24]. Furthermore, the transverse momenta of identified b jets are affected by the QCD radiation in the $H \to b\bar{b}$ decay, thus changing the fraction of decay products which pass kinematic cuts.

The first step toward a better understanding of the interplay between Higgs boson production and decay in WBF was made in Ref. [24], where both $H \to b\bar{b}$ and $H \to W^+W^- \to 4l$ decays were studied. It was found that imposing fiducial cuts on the Higgs boson decay products could change the NNLO QCD corrections by an order-one factor, making the impact of these cuts comparable to the size of the NNLO corrections themselves. In this reference, the WBF-production process was considered at NNLO QCD, but the decay $H \to b\bar{b}$ was treated at LO only. In the present paper, we extend the study of Ref. [24] and include QCD corrections to the Higgs boson decay as well, providing, for the first time, an NNLO-QCD-accurate description of the combined WBF process $pp \to H(\to b\bar{b})jj$. As we will show in this paper, the magnitude of radiative corrections to $pp \to H(\to b\bar{b})jj$ is significantly affected by the transverse momentum cut on b jets. We find that for the values of this cut used in recent analyses by the ATLAS and CMS Collaborations, the QCD corrections are significant, reducing the LO prediction by about 40%.

The remainder of the paper is organized as follows. In Sec. II we summarize the salient technical details of our calculation. We explain how corrections to the $H \to b\bar{b}$ decay are included in the calculation and discuss the approximations we employ. We present phenomenological results in Sec. III where we also investigate the origin of the fairly large QCD corrections that appear when Higgs boson decay to $b\bar{b}$ pairs is included in the calculation. We conclude in Sec. IV.

II. TECHNICAL DETAILS

We consider Higgs boson production in weak boson fusion $pp \to Hjj$ followed by the decay $H \to b\bar{b}$. The combined process is described in the narrow width approximation, which implies that the production and decay processes factorize, the Higgs boson is always on the mass shell, and the QCD corrections to the production and decay can be considered separately. We therefore write the differential cross section as

$$\mathrm{d}\sigma = \mathrm{Br}_{H\to b\bar{b}}\mathrm{d}\sigma_{\mathrm{WBF}}\mathrm{d}\gamma_b, \tag{1}$$

where $\mathrm{Br}_{H\to b\bar{b}}$ is the $H \to b\bar{b}$ branching ratio, $\mathrm{d}\sigma_{\mathrm{WBF}}$ is the differential WBF-production cross section, and $\mathrm{d}\gamma_b$ is the ratio of the differential and inclusive widths of the $H \to b\bar{b}$ decay

$$\mathrm{d}\gamma_b = \frac{\mathrm{d}\Gamma_b}{\Gamma_b}. \tag{2}$$

In principle, all quantities shown on the right-hand side in Eq. (1) receive QCD corrections, and the perturbative

[1]For earlier NLO QCD computations, see Refs. [14,15].

expansion of $d\sigma$ should involve all of them. However, since our focus in this paper is on how QCD corrections to the decay can impact the fiducial cross section, we decide to set $\mathrm{Br}_{H\to b\bar{b}}$ to a fixed value, $\mathrm{Br}_{H\to b\bar{b}} = 0.5824$ [25]. At the same time, if a discussion of perturbative convergence of $d\sigma$, including the perturbative expansion of $\mathrm{Br}_{H\to b\bar{b}}$, is desired, it can easily be constructed from the results that we present below. The last reason for writing the differential cross section as in Eq. (1) is that, for an observable that is inclusive in the decay products of the Higgs boson, the impact of the decay is captured by the branching ratio alone, because

$$\int d\gamma_b = 1. \tag{3}$$

We then proceed by separately expanding the quantities $d\sigma_{\mathrm{WBF}}$, $d\Gamma_b$, and Γ_b in α_s, following the prescription of Refs. [26–31]. Thus, denoting the ith term in the α_s expansion of a quantity X as $X^{(i)}$, with the appropriate power of α_s included in $X^{(i)}$, we construct an $\mathrm{N}^n\mathrm{LO}$ approximation of $d\sigma$,

$$d\sigma^{\mathrm{N}^n\mathrm{LO}} = \mathrm{Br}_{H\to b\bar{b}} \sum_{k=0}^{n} d\sigma_{\mathrm{WBF}}^{(n-k)} \times d\gamma^{\mathrm{N}^k\mathrm{LO}}, \tag{4}$$

where

$$d\gamma^{\mathrm{N}^n\mathrm{LO}} = \frac{\sum_{k=0}^{n} d\Gamma_b^{(k)}}{\Gamma_b^{\mathrm{N}^n\mathrm{LO}}}, \qquad \Gamma_b^{\mathrm{N}^n\mathrm{LO}} = \sum_{k=0}^{n} \Gamma_b^{(k)}. \tag{5}$$

We note that the quantities $d\gamma^{\mathrm{N}^n\mathrm{LO}}$ integrated over fiducial phase space describe a mismatch between corrections to inclusive and fiducial decay widths and, therefore, are very important for the discussion of the impact of QCD corrections to $H \to b\bar{b}$ decay on Higgs boson production in WBF in the presence of kinematic cuts on final-state particles.

Furthermore, although it would be legitimate to expand the inverse width in the definition of $d\gamma^{\mathrm{N}^n\mathrm{LO}}$ in a series in α_s, we decided not to do so because the NLO corrections to Γ_b are fairly large. Clearly, our results for $d\sigma^{\mathrm{N}^n\mathrm{LO}}$ are accurate up to and including $\mathcal{O}(\alpha_s^n)$. We will further discuss this and other alternatives for providing an NNLO prediction for the fiducial cross section in Sec. III.

The calculation of $d\sigma^{\mathrm{N}^n\mathrm{LO}}$, $n = 0, 1, 2$ does not require any new theoretical computation since fully differential descriptions of both $d\sigma_{\mathrm{WBF}}$ and $d\gamma$ through NNLO in perturbative QCD are available [24,32]. The latter computation was performed in the Higgs boson rest frame but, since the Higgs boson is a spin-zero particle, this is sufficient. We obtain the Higgs boson momentum from production kinematics, let it decay in its rest frame, and then boost the momenta of all particles that originate from Higgs boson decay to the laboratory frame where the WBF-production process occurs.

We emphasize that, although the step of combining theoretical predictions for Higgs boson production and decay in WBF is simple conceptually, doing so in practice requires care. Indeed, we need to interface the code for computing NNLO QCD corrections to the production described in Ref. [24] and the code for computing NNLO QCD corrections to $H \to b\bar{b}$ decay presented in Ref. [32]. Both codes produce fully differential results for the respective quantities through NNLO in perturbative QCD using local subtraction schemes. As a result, each subprocess comprises terms with varying multiplicities, weights, and four-momenta. Hence, we need to ensure that these quantities are properly combined such that selection criteria can be applied to the complete set of final-state particles in an infrared-safe way.

Another important aspect that needs to be addressed is the efficiency of the interfaced code. We have pointed out in Ref. [24] that the complexity of the NNLO QCD computation in the WBF process makes it difficult to consider complex decay products of the Higgs boson because the already-large dimensionality of the phase space becomes even larger. Since for processes of the deep-inelastic-scattering type—to which Higgs production in WBF belongs—the adaptation of the integration grids in higher-order computations may be a challenge, any increase in the dimensionality of the phase space may have a detrimental effect on the efficiency of the computation. In the current case, we have solved these problems by preparing dedicated integration grids for different parts of the calculation, using additional parameters to change the magnitude of certain subtraction terms, working with Message Passing Interface protocols to parallelize the computation, and simply using very large samples of points for Monte Carlo integration. Nevertheless, even with all these improvements, computational resources of roughly 5×10^5 CPU hours were required to produce the numerical results that we present in the next section.

Finally, since Higgs decays to b quarks in the WBF process are identified by the presence of two b jets in the final state, and since the identification of the flavor of jets in perturbative computations is subtle [33], it is important to note that the calculation of Ref. [32] is performed for *massive b* quarks. This has important consequences because it allows us to directly employ the standard anti-$k_\perp$ algorithm [34,35] to identify b jets in an infrared-safe manner.[2] However, we note that Higgs boson production in WBF is still computed with *massless b* quarks. We ensure infrared and collinear safety of our calculation by only

[2]As an alternative, we could perform the calculation using massless b quarks in the decay and either the flavor-$k_\perp$ algorithm [33] or one of the new-generation flavor-safe variants of the anti-$k_\perp$ algorithm [36–39].

considering b quarks from the decay subprocess in the flavor tagging, effectively treating b quarks originating from the production as flavorless. This makes our computation incomplete, and in order to complete it, one should also use massive quarks in the production process. However, as we argue below, at the end of Sec. III, the omitted effects are minor compared to the fiducial volume effects introduced by the inclusion of $H \to b\bar{b}$ decays in the theoretical predictions.

III. RESULTS

For numerical computations, we employ the standard setup that has been used to provide theoretical descriptions of weak boson fusion in the past [12,13,24]. We consider proton-proton collisions at 13 TeV center-of-mass energy. We set the mass of the Higgs boson to $m_H = 125$ GeV, the mass of the W boson to $m_W = 80.398$ GeV, and the mass of the Z boson to $m_Z = 91.1876$ GeV. As is customary, we include widths of electroweak gauge bosons in their propagators and choose $\Gamma_W = 2.1054$ GeV and $\Gamma_Z = 2.4952$ GeV for the numerical values, respectively.[3] Weak couplings are derived from the Fermi constant $G_F = 1.16639 \times 10^{-5}$ GeV^{-2} and the Cabibbo–Kobayashi–Maskawa (CKM) matrix is set to the identity matrix.[4]

The b-quark Yukawa coupling $\bar{y}_b$ is computed in the $\overline{\text{MS}}$ scheme [40] using the b-quark mass $\bar{m}_b(\mu = m_H) = 2.81$ GeV and the relation $\bar{y}_b = \bar{m}_b(2\sqrt{2}G_F)^{1/2}$. We use the package RunDec [41–43] to calculate the running at two-loop order using five active quark flavors. For the b-quark mass that appears in the matrix elements and in the phase space of $H \to b\bar{b}$ decay, we use the pole mass with a numerical value $m_b^{\text{pole}} = 4.78$ GeV. Furthermore, at NNLO, there is a contribution to $H \to b\bar{b}$ decays which is mediated by a top-quark loop [32,44–47]. To compute this contribution we use $m_t^{\text{pole}} = 173.2$ GeV; the top-quark Yukawa coupling is derived from this value as well, via $y_t = m_t^{\text{pole}}(2\sqrt{2}G_F)^{1/2}$.

With this setup, the $H \to b\bar{b}$ decay width for $\mu = m_H$ at different orders is

$$\begin{aligned} \Gamma_b^{\text{LO}} &= 1.926 \text{ MeV}, \\ \Gamma_b^{\text{NLO}} &= 2.327 \text{ MeV}, \\ \Gamma_b^{\text{NNLO}} &= 2.432 \text{ MeV}. \end{aligned} \tag{6}$$

The Monte Carlo integration uncertainties in the decay rate Γ_b are negligible in comparison to the Monte Carlo uncertainty in the fiducial cross section σ. Although these decay widths were computed using the same code as was used in Ref. [32], they are slightly different from the results presented there due to somewhat different choices of input parameters, most notably the top-quark Yukawa coupling.

We employ NNPDF31_nnlo_as_0118 parton distribution functions [48] and $\alpha_s(m_Z) = 0.118$ for all calculations reported below. The evolution of both parton distribution functions and the strong coupling constant is obtained directly from LHAPDF [49]. We use equal renormalization and factorization scales to describe Higgs boson production in WBF. As a central scale, we choose [12]

$$\mu_0^2 = \frac{m_H}{2}\sqrt{\frac{m_H^2}{4} + p_{\perp,H}^2}, \tag{7}$$

where $p_{\perp,H}$ is the *true* Higgs boson transverse momentum. To study the dependence of theoretical predictions on the renormalization and factorization scales, we compute them for $\mu_R = \mu_F = 2\mu_0$ and $\mu_R = \mu_F = \mu_0/2$. We choose $\mu = m_H$ as our central scale for the Higgs boson decay subprocess. We will not investigate the impact of the scale variation in the decay systematically, but we will make some comments about how such a choice impacts theoretical predictions.

Final-state jets, including b jets, are defined using the standard anti-$k_\perp$ algorithm [34,35] with a jet radius parameter of $R = 0.4$. We select events that have at least two b jets in the final state, where, following the ATLAS analysis in Ref. [7], each of the b jets is required to have a transverse momentum $p_{\perp,b} > 65$ GeV and a rapidity $|y_b| < 2.5$. We remind the reader that in our calculation, b jets come *exclusively* from Higgs boson decays. Most of our events have, therefore, at most two b jets, although signatures with four b jets may arise due to the NNLO corrections to the decay. In this case, we consider the two b jets with an invariant mass that is closest to the mass of the Higgs boson as a candidate pair to reconstruct the Higgs boson momentum. If more than one b and/or $\bar{b}$ quark are clustered into a jet, we still call it a b jet and include it in the b-jet counting. It is clear that there is a certain ambiguity in how such multiple b tags should be handled, but the whole effect is small and does not change the overall pattern of radiative corrections that we describe below.

Once two b jets that reconstruct the Higgs boson are identified, we apply standard WBF cuts to the remaining jets, which we will refer to as "light jets."[5] Specifically, we require that a WBF event contains at least two light jets with transverse momenta $p_{\perp,j} > 25$ GeV and rapidities $|y_j| < 4.5$. The two leading-$p_\perp$ light jets must have well-separated rapidities $|y_{j_1} - y_{j_2}| > 4.5$, and their invariant mass should be at least 600 GeV. In addition, the two

[3]The widths in the propagators of gauge bosons are included only for consistency with previous calculations. They are treated as scale-independent constants; i.e., we do not use the complex mass scheme.

[4]This does not affect the predictions because of CKM unitarity and the fact that we treat all the light jets in the production on equal footing.

[5]Note that the light jets may arise from radiative corrections to either the production or decay process.

leading light jets must be in opposite hemispheres in the laboratory frame; this is enforced by requiring that the product of their rapidities in the laboratory frame is negative, $y_{j_1} y_{j_2} < 0$.

We are now in the position to present the results of the calculation. We start by computing fiducial cross sections at LO, NLO, and NNLO in the perturbative QCD expansion. We find[6]

$$\begin{aligned}\sigma^{\rm LO} &= 75.6^{-5.6}_{+6.5}\ \text{fb},\\ \sigma^{\rm NLO} &= 52.4^{+1.5}_{-2.6}\ \text{fb},\\ \sigma^{\rm NNLO} &= 44.6^{+0.9}_{-0.6}\ \text{fb},\end{aligned} \tag{8}$$

where the superscripts and subscripts indicate values with $\mu_R = \mu_F = 2\mu_0$ and $\mu_R = \mu_F = \mu_0/2$, respectively. Monte Carlo integration uncertainties are about a few permille and thus much smaller than the residual scale uncertainties; consequently, we do not show them. The results in Eq. (8) show that, compared to the LO cross section, the NLO cross section is reduced by about 30% and the NNLO cross section by an additional 10%. These significant corrections should be contrasted with the scale uncertainties, which are about 9%, 5%, and 2% on the LO, NLO, and NNLO predictions, respectively. Hence, in this case, the strategy of estimating uncertainties of theoretical predictions by studying their sensitivity to renormalization and factorization scales does not capture the contributions from missing higher orders.

The large negative QCD corrections seen in Eq. (8) arise because corrections to the decay in the fiducial region are different from those to the inclusive width and, while they are moderate in both cases, they conspire to reduce the fiducial cross section. We will now illustrate this statement by considering the different contributions that lead to the results shown in Eq. (8).

It follows from Eqs. (4) and (5) that higher-order QCD corrections to the differential WBF cross section with $H \to b\bar{b}$ decay originate from the interplay of three different contributions: the radiative corrections to the WBF-production process $\mathrm{d}\sigma_{\rm WBF}$, the radiative corrections to the differential decay process $\mathrm{d}\Gamma_b$, and the expansion of the total $H \to b\bar{b}$ width Γ_b in α_s. We will refer to these corrections as $\Delta_{\rm prod}$, $\Delta_{\rm dec}$, and $\Delta_{\rm exp}$, respectively. Beyond LO, we write the cross section Eq. (4) as

$$\mathrm{d}\sigma^{\mathrm{N}^n\mathrm{LO}} = \mathrm{d}\sigma^{\rm LO} + \sum_{k=1}^{n} \mathrm{d}\Delta^{\mathrm{N}^k\mathrm{LO}}. \tag{9}$$

We write

$$\begin{aligned}\mathrm{d}\Delta^{\rm NLO} &= \mathrm{d}\Delta^{(1,0)}_{\rm prod} + \mathrm{d}\Delta^{(0,1)}_{\rm dec} + \mathrm{d}\Delta^{(0,1)}_{\rm exp},\\ \mathrm{d}\Delta^{\rm NNLO} &= \mathrm{d}\Delta^{(2,0)}_{\rm prod} + \mathrm{d}\Delta^{(1,1)}_{\rm dec} + \mathrm{d}\Delta^{(0,2)}_{\rm dec}\\ &\quad + \mathrm{d}\Delta^{(1,1)}_{\rm exp} + \mathrm{d}\Delta^{(0,2)}_{\rm exp}.\end{aligned} \tag{10}$$

The individual contributions are defined as

$$\begin{aligned}\mathrm{d}\Delta^{(1,0)}_{\rm prod} &= \mathrm{Br}_{H\to b\bar{b}}\left(\mathrm{d}\sigma^{(1)}_{\rm WBF} \times \frac{\mathrm{d}\Gamma^{(0)}_b}{\Gamma^{(0)}_b}\right),\\ \mathrm{d}\Delta^{(0,1)}_{\rm dec} &= \mathrm{Br}_{H\to b\bar{b}}\frac{\Gamma^{(1)}_b}{\Gamma^{\rm NLO}_b}\left(\mathrm{d}\sigma^{(0)}_{\rm WBF} \times \frac{\mathrm{d}\Gamma^{(1)}_b}{\Gamma^{(1)}_b}\right),\\ \mathrm{d}\Delta^{(0,1)}_{\rm exp} &= -\mathrm{Br}_{H\to b\bar{b}}\frac{\Gamma^{(1)}_b}{\Gamma^{\rm NLO}_b}\left(\mathrm{d}\sigma^{(0)}_{\rm WBF} \times \mathrm{d}\gamma^{\rm LO}\right),\end{aligned} \tag{11}$$

and

$$\begin{aligned}\mathrm{d}\Delta^{(2,0)}_{\rm prod} &= \mathrm{Br}_{H\to b\bar{b}}\left(\mathrm{d}\sigma^{(2)}_{\rm WBF} \times \frac{\mathrm{d}\Gamma^{(0)}_b}{\Gamma^{(0)}_b}\right),\\ \mathrm{d}\Delta^{(1,1)}_{\rm dec} &= \mathrm{Br}_{H\to b\bar{b}}\frac{\Gamma^{(1)}_b}{\Gamma^{\rm NLO}_b}\left(\mathrm{d}\sigma^{(1)}_{\rm WBF} \times \frac{\mathrm{d}\Gamma^{(1)}_b}{\Gamma^{(1)}_b}\right),\\ \mathrm{d}\Delta^{(0,2)}_{\rm dec} &= \mathrm{Br}_{H\to b\bar{b}}\frac{\Gamma^{(2)}_b}{\Gamma^{\rm NNLO}_b}\left(\mathrm{d}\sigma^{(0)}_{\rm WBF} \times \frac{\mathrm{d}\Gamma^{(2)}_b}{\Gamma^{(2)}_b}\right),\\ \mathrm{d}\Delta^{(1,1)}_{\rm exp} &= -\mathrm{Br}_{H\to b\bar{b}}\frac{\Gamma^{(1)}_b}{\Gamma^{\rm NLO}_b}\left(\mathrm{d}\sigma^{(1)}_{\rm WBF} \times \mathrm{d}\gamma^{\rm LO}\right),\\ \mathrm{d}\Delta^{(0,2)}_{\rm exp} &= -\mathrm{Br}_{H\to b\bar{b}}\frac{\Gamma^{(2)}_b}{\Gamma^{\rm NNLO}_b}\left(\mathrm{d}\sigma^{(0)}_{\rm WBF} \times \mathrm{d}\gamma^{\rm NLO}\right).\end{aligned} \tag{12}$$

We choose $\mu_{\rm R} = \mu_{\rm F} = \mu_0$, integrate over the fiducial phase space, and find

$$\begin{aligned}\Delta^{(1,0)}_{\rm prod} &= -4.9\ \text{fb}, & \Delta^{(0,1)}_{\rm dec} &= -5.3\ \text{fb},\\ \Delta^{(0,1)}_{\rm exp} &= -13.0\ \text{fb},\\ \Delta^{(2,0)}_{\rm prod} &= -1.5\ \text{fb}, & \Delta^{(1,1)}_{\rm dec} &= +0.4\ \text{fb},\\ \Delta^{(0,2)}_{\rm dec} &= -5.0\ \text{fb}, & \Delta^{(1,1)}_{\rm exp} &= +0.8\ \text{fb},\\ \Delta^{(0,2)}_{\rm exp} &= -2.5\ \text{fb}.\end{aligned} \tag{13}$$

It follows from Eqs. (8) and (13) that the corrections arising from the production process ($\Delta^{(1,0)}_{\rm prod}$ and $\Delta^{(2,0)}_{\rm prod}$) are small and negative; they amount to approximately -6% at NLO and -2% at NNLO, and hence are covered by scale uncertainty estimates. These corrections were extensively discussed in Ref. [24]. The corrections associated with the differential decay process ($\Delta^{(0,1)}_{\rm dec}$ and $\Delta^{(0,2)}_{\rm dec}$) are both about -7% of the LO cross section, indicating that the perturbative expansion

[6]The small difference in the LO cross section compared to the result reported in Ref. [24] is due to the inclusion of the nonzero b-quark mass in $H \to b\bar{b}$ decays in this computation.

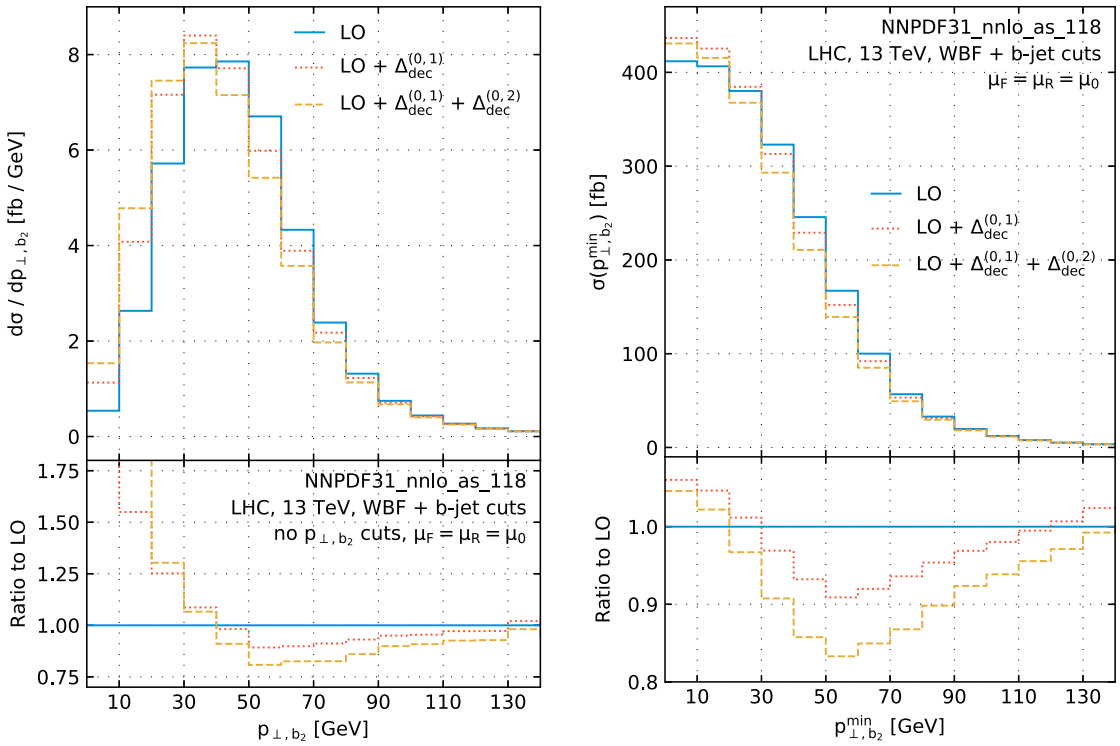

FIG. 1. The impact of QCD corrections to the $H \to b\bar{b}$ decay on the transverse momentum distribution of the subleading b jet (left) and on the fiducial cross section defined in Eq. (14) (right). In each plot, the upper pane shows results at LO, NLO, and NNLO in the decay process, while the Higgs boson production process is kept at LO QCD. The lower panes show the ratio with respect to the LO results. See text for details.

does not seem to converge. Moreover, since they are also negative, they amplify corrections to the production. We study these rather large corrections in more detail below.

Before doing so, we note that the corrections arising from the expansion of the width Γ_b, which appears in the definition of the cross section through Eq. (5), are significant and also negative. At NLO they lead to a large decrease in the fiducial cross section shown in Eq. (8). At NNLO, however, the corrections from expanding Γ_b are negative but moderate, giving an overall decrease of the cross section by about 2% with respect to the LO value. Thus, we conclude that the reason for large QCD corrections to the WBF process with Higgs boson decay to a $b\bar{b}$ pair is the fact that a number of moderately large negative corrections amplify each other and lead to a significant decrease in the fiducial cross section when taken together.

The feature of NNLO QCD corrections that clearly stands out is the lack of apparent convergence of the perturbative expansion of the decay width $H \to b\bar{b}$ in the fiducial volume. To understand this feature better, we note that the cut on the transverse momenta of the two b jets, $p_{\perp,b} \geq 65$ GeV, is rather high as it exceeds $m_H/2$. Hence, if the Higgs bosons were produced with zero transverse momentum, none of the b jets from Higgs boson decays would pass this cut. Of course, this does not happen in WBF since the typical transverse momentum of Higgs bosons in this process is $p_{\perp,H} \approx 120$ GeV. Because of this, it may appear that the cut on the b-jet transverse momentum is sufficiently low to leave a fiducial phase space that is large enough for perturbative stability. However, as we will show below, this is not the case, and this cut appears to be too restrictive from the point of view of perturbative convergence.

To illustrate this point, we recompute the decay corrections $\Delta^{(0,i)}_{\text{dec}}$, $i = 1, 2$, imposing all fiducial cuts except the transverse momentum cut on the subleading b jet, $p^{\text{min}}_{\perp,b_2}$, and study the transverse momentum distribution of this jet up to NNLO. The results are shown in Fig. 1. The distribution peaks around $p_{\perp,b_2} \approx 30$ GeV and then decreases quite rapidly between 40 and 80 GeV. The additional real emissions in the process $H \to b\bar{b}$ tend to reduce the transverse momentum of b jets from Higgs boson decay, making their transverse momentum distribution softer. QCD corrections to the right of the peak converge poorly, with NLO and NNLO contributions being moderate but quite comparable without clear hierarchy. Only to the left of the peak at $p_{\perp,b_2} \approx 30$ GeV do the corrections start exhibiting signs of perturbative convergence.

To emphasize this point, we show the cumulative distribution, i.e.,

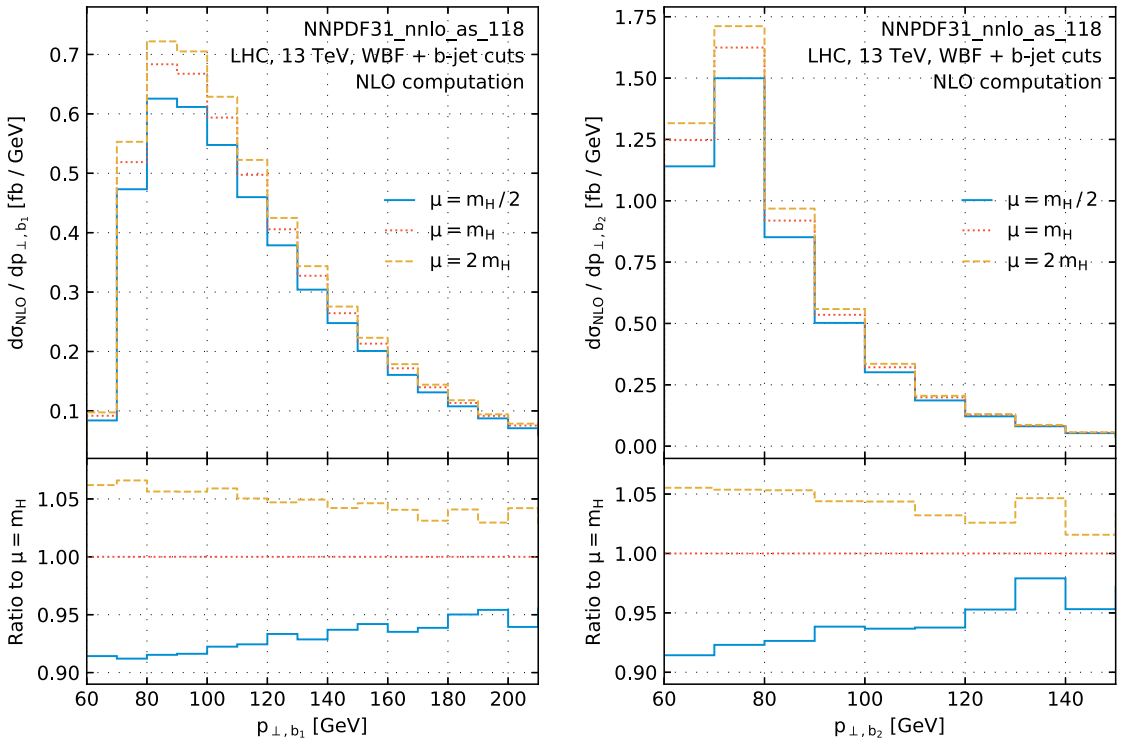

FIG. 2. Distributions of transverse momenta of the leading (left) and subleading (right) b jets. In each plot, the upper pane shows the NLO computation for different renormalization scales used in the computation of the $H \to b\bar{b}$ decay width. In all these results, the central scale choice is used for the renormalization and factorization scale in the Higgs boson production process. The lower pane shows the ratio to the central scale choice $\mu = m_H$. See text for details.

$$\sigma(p_{\perp,b_2}^{\min}) = \int_{p_{\perp,b_2}^{\min}}^{\infty} \mathrm{d}p_{\perp,b_2} \frac{\mathrm{d}\sigma}{\mathrm{d}p_{\perp,b_2}} \tag{14}$$

in the right pane in Fig. 1, from which one can infer the dependence of the fiducial cross section on the lower cut on $p_{\perp,b_2}$. We emphasize that only corrections to the decay are included in the cross sections shown in that figure. We observe that for $p_{\perp,b_2}^{\min} \gtrsim 30$ GeV the NLO and NNLO corrections are comparable in size and the perturbative convergence is quite poor; QCD corrections to the fiducial decay width start converging only for smaller values of this cut.

Since it is clear that the cut on $p_{\perp,b}$ plays an important role in separating the $H \to b\bar{b}$ signal for the background, relaxing it dramatically is not an option. On the other hand, we observe that the cut on the subleading b jet is primarily responsible for the poor perturbative convergence. This suggests that it might be possible to keep a stringent cut on $p_{\perp,b_1}$ while relaxing that on $p_{\perp,b_2}$, allowing the discrimination of signal and background without ruining perturbative convergence. Of course, this would require detailed studies, which are beyond the scope of this paper.

As we already mentioned, the second source of large corrections comes from the expansion of the inclusive partial decay width Γ_b in the denominator in Eq. (2); the NLO correction from this expansion changes the fiducial cross section by -17% in comparison to LO. This is a consequence of the relatively large corrections to the partial width; cf. Eq. (6).

It was observed in Ref. [32] that corrections to the width converge somewhat faster if the renormalization scale $\mu = m_H/2$ for the decay is chosen. However, we do not see a clear benefit for using this scale in the WBF computation. Indeed, for $\mu = m_H/2$, we find $\Delta_{\mathrm{exp}}^{(0,1)} = -8.3$ fb and $\Delta_{\mathrm{dec}}^{(0,1)} = -13.8$ fb. The two corrections add up to -22.1 fb which should be compared to a similar result of -18.3 fb for $\mu = m_H$.[7] Hence, for $\mu = m_H/2$, corrections to $\mathrm{d}\sigma$ are somewhat larger than for $\mu = m_H$ and, more generally, the impact of the scale variation in the decay is comparable to that in the production. The same conclusions can be drawn from the impact of decay scale variations on differential distributions. This statement is illustrated in Fig. 2, where only NLO results are shown. We do this to verify that decay scale variations cannot capture the observed large shifts due to higher-order QCD corrections; because of that, we see no point in further pursuing detailed studies of the scale variation in the decay.

[7]We note that $\mathrm{d}\gamma^{\mathrm{LO}}$, $\mathrm{d}\sigma^{\mathrm{LO}}$, and $\mathrm{d}\Delta_{\mathrm{prod}}^{(1,0)}$ are independent of the renormalization scale in the decay.

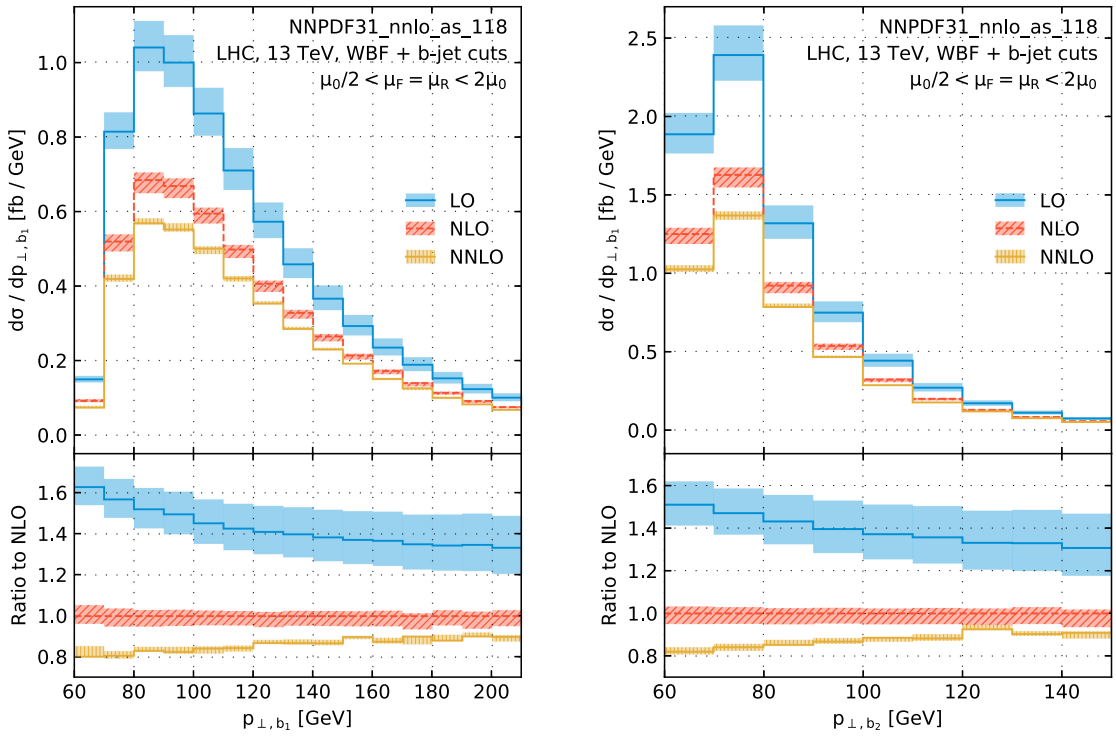

FIG. 3. Transverse momentum distributions of the leading (left) and subleading (right) b jets. In each plot, the upper pane shows the LO, NLO, and NNLO QCD computations. The lines indicate the central renormalization and factorization scale choice, while the envelopes around them indicate the range of results for different scales in the production process. The lower panes show the ratios with respect to the NLO results at central scale. See text for details.

As noted earlier, there are different ways of combining the branching ratio $\mathrm{Br}_{H\to b\bar{b}}$ with the quantity $\mathrm{d}\sigma_{\mathrm{WBF}} \times \mathrm{d}\gamma$. In doing so, we need to remember that the formula in Eq. (1) is obtained by rewriting $\mathrm{d}\Gamma_b/\Gamma_H$ as the product of $\mathrm{Br}_{H\to b\bar{b}}$ and $\mathrm{d}\gamma = \mathrm{d}\Gamma_b/\Gamma_b$, and that the total width Γ_b also appears in the numerator of $\mathrm{Br}_{H\to b\bar{b}}$. Hence, if we choose to expand $\mathrm{Br}_{H\to b\bar{b}}$ in α_s, we must ensure that the total width Γ_b is treated in the same way in both $\mathrm{Br}_{H\to b\bar{b}}$ and $\mathrm{d}\gamma$. For the prescription that we employ in this paper, this treatment works such that the quantity $\mathrm{d}\sigma^{\mathrm{NNLO}}$ is accurate up to and including $\mathcal{O}(\alpha_s^2)$. We note that other ways to construct the NNLO value for $\mathrm{d}\sigma$, for example, expanding the inverse width $1/\Gamma_b$ in α_s or the prescription discussed in Ref. [50], result in predictions for cross sections that differ from the NNLO result shown in Eq. (8) by about 2 fb.

We continue with the discussion of QCD corrections to kinematic distributions in the WBF process for fiducial cuts (including $p_{\perp,b_2} > 65$ GeV). We begin with displaying the transverse momentum of the leading and subleading b jets in Fig. 3. The main effect of the higher-order QCD corrections on these distributions is a nearly uniform reduction of the LO results by an amount that is comparable to that of the fiducial cross section. This can be clearly seen from the ratio to NLO shown in the lower panes. The NLO K factors increase slightly from around $1/1.6 \approx 0.6$ for low values of $p_\perp$ to around $1/1.3 \approx 0.8$ in the tails of the distributions. No significant modifications of differential K factors at NNLO are observed, so that the shape changes of these distributions are well captured by NLO predictions.[8]

The situation changes, however, if we consider the transverse momentum distributions of the two b jets whose invariant mass is closest to the Higgs boson mass, which can be interpreted as the transverse momentum of the "reconstructed" Higgs boson. This distribution is shown in the left pane in Fig. 4. We observe that in this case, both the NLO and NNLO K factors are rapidly changing functions of the transverse momentum, with the NLO K factor taking a value of around $1/2.4 \approx 0.4$ at $p_{\perp,bb} = 70$ GeV, rising rapidly to about $1/1.4 \approx 0.7$ at $p_{\perp,bb} = 150$ GeV, and leveling off after that. We also observe a more significant difference between NNLO and NLO distributions as compared to the $p_\perp$ distributions of individual jets. This behavior is caused by a strong correlation between the value of the (true) Higgs boson transverse momentum and the ability of the produced b jets to pass the cuts, especially when additional QCD radiation is considered.

[8]We note that similar to the fiducial cross sections discussed in Eq. (8), the scale-variation bands for transverse momentum distributions in consecutive perturbative orders do not overlap either.

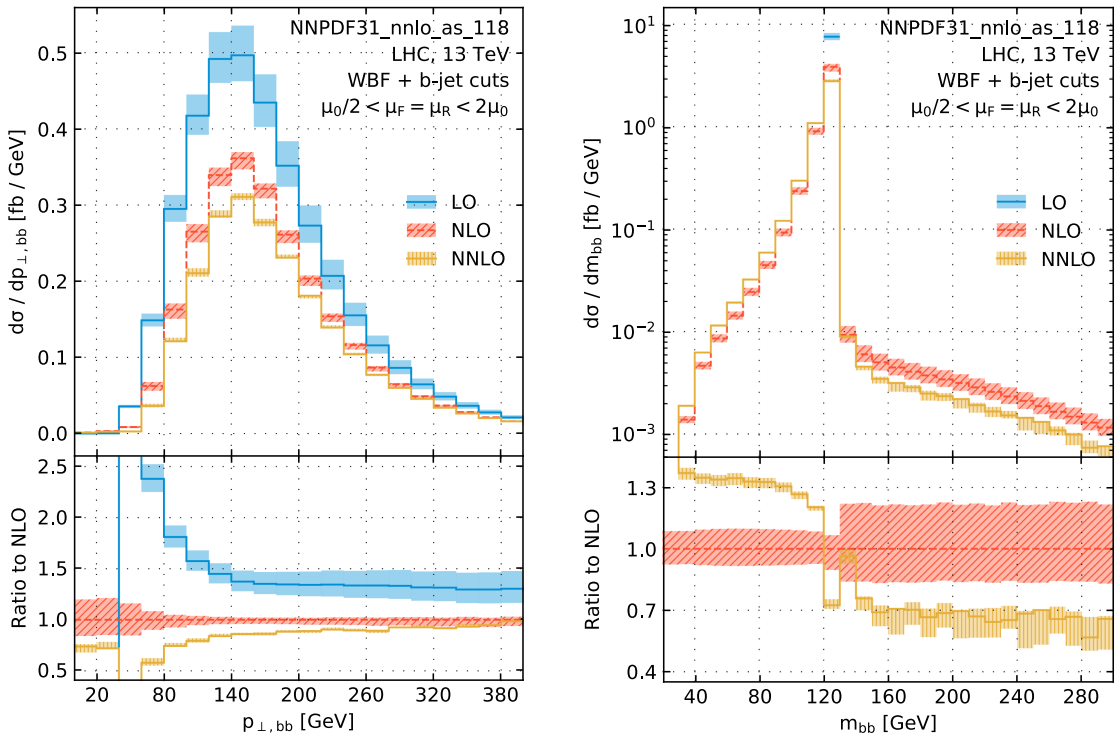

FIG. 4. Distributions of the transverse momentum (left) and the invariant mass of the reconstructed Higgs boson (right). See caption of Fig. 3 and text for details.

Another distribution that is interesting to discuss is the invariant mass distribution of the two reconstructed b jets, m_{bb}; it is shown in the right pane of Fig. 4. In the absence of QCD radiation in the decay and when no interplay between production and decay is considered, this distribution populates a single bin because the momenta of two b jets always reconstruct the mass of the Higgs boson. However, when radiative corrections are considered and final-state partons from the production process and Higgs boson decay are treated on an equal footing, the invariant mass distribution of the two b jets is altered significantly.

As follows from the right pane in Fig. 4, there is a tail to the left of $m_{bb} = m_H$ caused by the QCD radiation in the decay, and a tail to the right caused by the fact that occasionally the QCD radiation in production and one of the b quarks from $H \to b\bar{b}$ decay are combined. Note that the "left" tail exhibits large positive NNLO contributions as more and more events populate this region.

This plot allows us to indirectly address the issue of whether it is justifiable to disregard b jets from the production. We can estimate the significance of clustering partons from production and partons from decays into the b jets by counting the number of events with an invariant mass m_{bb} above m_H and comparing it to the total number of Higgs bosons produced. We find that the number of such events is about 1% of the total and that it is not drastically affected by the NNLO QCD corrections. We may interpret this result as a measure of how often one of the b quarks from Higgs boson decay and *any* of the partons from the production find themselves sufficiently close to each other to be clustered into a jet. Since in this article we did not consider production of b jets in the weak boson fusion process proper, this result gives us an estimate of how often partons from the production process end up in the "decay" fiducial region.

Furthermore, by considering simple LO processes, we have estimated that additional b jets are present in roughly 1% of events that contribute to the fiducial WBF cross sections in Eq. (8). This is negligible compared to the magnitude of QCD corrections that are discussed in this paper. It would also be easy to mitigate the effect of b jets from the production subprocess with even a loose cut on the invariant mass of two b jets, requiring it to select events which are sufficiently close to m_H. In this case, the impact of b quarks from the WBF-production subprocess on the cross section with $H \to b\bar{b}$ decay would be further reduced. We take these observations as an indication that the impact of treating b quarks from the production process as effectively unflavored should not qualitatively alter our findings.

IV. CONCLUSIONS

Fiducial cross sections for Higgs boson production in weak boson fusion show bad perturbative convergence if scale uncertainties are used as a criterion for estimating

higher-order QCD corrections [12,13]. Considering the $H \to b\bar{b}$ decay at leading order, it was observed that additional b-jet selection criteria restrict the fiducial WBF region and improve the perturbative convergence [24]. However, an important effect, QCD radiation in the decay, was not included in that paper.

In the current paper, we extended that study by considering Higgs boson production in WBF followed by the decay of the Higgs boson into a pair of b quarks, treating both production and decay at NNLO QCD. We found that WBF cross sections measured in the fiducial region akin to the one defined in Ref. [6] are subject to large perturbative corrections, which reduce the LO cross section by about 40%. This large reduction appears as a result of a number of moderate effects that amplify each other. As a consequence, conclusions about the improved perturbative convergence reached in [24] no longer hold, at least for the set of cuts on b jets that we studied.

The transverse momentum cut on b jets seems to play an important role in this because it causes QCD corrections to the $H \to b\bar{b}$ fiducial partial decay width to be large and different from the corrections to the inclusive one. Hence, if one hopes to use the $H \to b\bar{b}$ decay mode in WBF production to study the b-quark Yukawa coupling, it is crucial to control QCD corrections not only in the production subprocess but also to the decay. For better stability of perturbative computations, reducing the transverse momentum cut on b jets appears to be useful, but whether this is possible given the fact that this will bring in additional backgrounds, requires a separate investigation.

Alternatively, one can try to resum perturbative corrections to the decay and/or match the result of this calculation to a parton shower. It would be interesting to see whether the observed lack of perturbative stability in the decay of the Higgs boson subject to fiducial constraints will persist once the soft radiation is treated to all orders. As there is no color reconnection between production and decay processes, there should not be any conceptual obstacle to implementing such a calculation [51–53], which we intend on doing in the near future.

Finally, we note that a formal completion of the computation presented here would require modifying the existing NNLO computation for Higgs boson production in WBF to include the effect of massive b quarks. While some parts of such a calculation are straightforward, the most nontrivial part will require a computation of NLO QCD correction to the case when a gluon splits into a $b\bar{b}$ pair and then one of the b quarks from the splitting participates in the WBF process. Such a calculation is definitely doable but, given the magnitude of the corrections found in this paper, it is highly unlikely to change our conclusions.

ACKNOWLEDGMENTS

We want to thank Wojciech Bizoń for a fruitful collaboration on the calculation of NNLO QCD corrections to $H \to b\bar{b}$, which we relied upon in this paper. K. A. thanks Brookhaven National Laboratory, where a significant part of this research was conducted. R. R. has been partially supported by the Italian Ministry of Universities and Research through Grant No. PRIN 2022BCXSW9. The research of K. M. and I. N. is partially supported by the Deutsche Forschungsgemeinschaft (German Research Foundation) under Grant No. 396021762—TRR 257.

[1] A. Tumasyan *et al.* (CMS Collaboration), A portrait of the Higgs boson by the CMS experiment ten years after the discovery, Nature (London) **607**, 60 (2022); **623**, E4 (2023).

[2] G. Aad *et al.* (ATLAS Collaboration), A detailed map of Higgs boson interactions by the ATLAS experiment ten years after the discovery, Nature (London) **607**, 52 (2022); **612**, E24 (2022).

[3] J. M. Butterworth, A. R. Davison, M. Rubin, and G. P. Salam, Jet substructure as a new Higgs search channel at the LHC, Phys. Rev. Lett. **100**, 242001 (2008).

[4] A. M. Sirunyan *et al.* (CMS Collaboration), Evidence for the Higgs boson decay to a bottom quark-antiquark pair, Phys. Lett. B **780**, 501 (2018).

[5] A. M. Sirunyan *et al.* (CMS Collaboration), Observation of Higgs boson decay to bottom quarks, Phys. Rev. Lett. **121**, 121801 (2018).

[6] M. Aaboud *et al.* (ATLAS Collaboration), Evidence for the $H \to b\bar{b}$ decay with the ATLAS detector, J. High Energy Phys. 12 (2017) 024.

[7] M. Aaboud *et al.* (ATLAS Collaboration), Observation of $H \to b\bar{b}$ decays and VH production with the ATLAS detector, Phys. Lett. B **786**, 59 (2018).

[8] G. Aad *et al.* (ATLAS Collaboration), Measurements of Higgs bosons decaying to bottom quarks from vector boson fusion production with the ATLAS experiment at $\sqrt{s} = 13$ TeV, Eur. Phys. J. C **81**, 537 (2021).

[9] G. Aad *et al.* (ATLAS Collaboration), Search for Higgs boson production in association with a high-energy photon via vector-boson fusion with decay into bottom quark pairs at $\sqrt{s} = 13$ TeV with the ATLAS detector, J. High Energy Phys. 03 (2021) 268.

[10] A. Hayrapetyan *et al.* (CMS Collaboration), Measurement of the Higgs boson production via vector boson fusion and

its decay into bottom quarks in proton-proton collisions at $\sqrt{s} = 13$ TeV, J. High Energy Phys. 01 (2024) 173.
[11] CMS Collaboration, Search for boosted Higgs bosons produced via vector boson fusion in the $H \to b\bar{b}$ decay mode using LHC proton-proton collision data at $\sqrt{s} =$ 13 TeV, Report No. CMS-PAS-HIG-21-020, 2023.
[12] M. Cacciari, F. A. Dreyer, A. Karlberg, G. P. Salam, and G. Zanderighi, Fully differential vector-boson-fusion Higgs production at next-to-next-to-leading order, Phys. Rev. Lett. **115**, 082002 (2015); **120**, 139901(E) (2018).
[13] J. Cruz-Martinez, T. Gehrmann, E. W. N. Glover, and A. Huss, Second-order QCD effects in Higgs boson production through vector boson fusion, Phys. Lett. B **781**, 672 (2018).
[14] T. Figy, C. Oleari, and D. Zeppenfeld, Next-to-leading order jet distributions for Higgs boson production via weak boson fusion, Phys. Rev. D **68**, 073005 (2003).
[15] E. L. Berger and J. M. Campbell, Higgs boson production in weak boson fusion at next-to-leading order, Phys. Rev. D **70**, 073011 (2004).
[16] F. A. Dreyer and A. Karlberg, Vector-boson fusion Higgs production at three loops in QCD, Phys. Rev. Lett. **117**, 072001 (2016).
[17] M. Ciccolini, A. Denner, and S. Dittmaier, Strong and electroweak corrections to the production of Higgs + 2jets via weak interactions at the LHC, Phys. Rev. Lett. **99**, 161803 (2007).
[18] M. Ciccolini, A. Denner, and S. Dittmaier, Electroweak and QCD corrections to Higgs production via vector-boson fusion at the LHC, Phys. Rev. D **77**, 013002 (2008).
[19] T. Liu, K. Melnikov, and A. A. Penin, Nonfactorizable QCD effects in Higgs boson production via vector boson fusion, Phys. Rev. Lett. **123**, 122002 (2019).
[20] F. A. Dreyer, A. Karlberg, and L. Tancredi, On the impact of non-factorisable corrections in VBF single and double Higgs production, J. High Energy Phys. 10 (2020) 131; 04 (2022) 009(E).
[21] C. Brønnum-Hansen, M.-M. Long, and K. Melnikov, Scale dependence of non-factorizable virtual corrections to Higgs boson production in weak boson fusion, J. High Energy Phys. 11 (2023) 130.
[22] M.-M. Long, K. Melnikov, and J. Quarroz, Non-factorizable virtual corrections to Higgs boson production in weak boson fusion beyond the eikonal approximation, J. High Energy Phys. 07 (2023) 035.
[23] K. Asteriadis, C. Brønnum-Hansen, and K. Melnikov, Nonfactorizable corrections to Higgs boson production in weak boson fusion, Phys. Rev. D **109**, 014031 (2024).
[24] K. Asteriadis, F. Caola, K. Melnikov, and R. Röntsch, NNLO QCD corrections to weak boson fusion Higgs boson production in the $H \to b\bar{b}$ and $H \to WW^* \to 4l$ decay channels, J. High Energy Phys. 02 (2022) 046.
[25] D. de Florian *et al.* (LHC Higgs Cross Section Working Group), *Handbook of LHC Higgs Cross Sections: 4. Deciphering the Nature of the Higgs Sector*, CERN Yellow Reports: Monographs (CERN, Geneva, 2016), Vol. 2/2017, 10.23731/CYRM-2017-002.
[26] G. Ferrera, M. Grazzini, and F. Tramontano, Higher-order QCD effects for associated WH production and decay at the LHC, J. High Energy Phys. 04 (2014) 039.
[27] G. Ferrera, M. Grazzini, and F. Tramontano, Associated ZH production at hadron colliders: The fully differential NNLO QCD calculation, Phys. Lett. B **740**, 51 (2015).
[28] J. M. Campbell, R. K. Ellis, and C. Williams, Associated production of a Higgs boson at NNLO, J. High Energy Phys. 06 (2016) 179.
[29] G. Ferrera, G. Somogyi, and F. Tramontano, Associated production of a Higgs boson decaying into bottom quarks at the LHC in full NNLO QCD, Phys. Lett. B **780**, 346 (2018).
[30] F. Caola, G. Luisoni, K. Melnikov, and R. Röntsch, NNLO QCD corrections to associated WH production and $H \to b\bar{b}$ decay, Phys. Rev. D **97**, 074022 (2018).
[31] A. Behring, W. Bizoń, F. Caola, K. Melnikov, and R. Röntsch, Bottom quark mass effects in associated WH production with the $H \to b\bar{b}$ decay through NNLO QCD, Phys. Rev. D **101**, 114012 (2020).
[32] A. Behring and W. Bizoń, Higgs decay into massive b-quarks at NNLO QCD in the nested soft-collinear subtraction scheme, J. High Energy Phys. 01 (2020) 189.
[33] A. Banfi, G. P. Salam, and G. Zanderighi, Infrared safe definition of jet flavor, Eur. Phys. J. C **47**, 113 (2006).
[34] M. Cacciari, G. P. Salam, and G. Soyez, The anti-k_t jet clustering algorithm, J. High Energy Phys. 04 (2008) 063.
[35] M. Cacciari, G. P. Salam, and G. Soyez, FASTJET user manual, Eur. Phys. J. C **72**, 1896 (2012).
[36] S. Caletti, A. J. Larkoski, S. Marzani, and D. Reichelt, Practical jet flavour through NNLO, Eur. Phys. J. C **82**, 632 (2022).
[37] M. Czakon, A. Mitov, and R. Poncelet, Infrared-safe flavoured anti-k_T jets, J. High Energy Phys. 04 (2023) 138.
[38] R. Gauld, A. Huss, and G. Stagnitto, Flavor identification of reconstructed hadronic jets, Phys. Rev. Lett. **130**, 161901 (2023); **132**, 159901(E) (2024).
[39] F. Caola, R. Grabarczyk, M. L. Hutt, G. P. Salam, L. Scyboz, and J. Thaler, Flavored jets with exact anti-k_t kinematics and tests of infrared and collinear safety, Phys. Rev. D **108**, 094010 (2023).
[40] E. Braaten and J. P. Leveille, Higgs boson decay and the running mass, Phys. Rev. D **22**, 715 (1980).
[41] K. G. Chetyrkin, J. H. Kühn, and M. Steinhauser, RUNDEC: A MATHEMATICA package for running and decoupling of the strong coupling and quark masses, Comput. Phys. Commun. **133**, 43 (2000).
[42] B. Schmidt and M. Steinhauser, CRUNDEC: A C++ package for running and decoupling of the strong coupling and quark masses, Comput. Phys. Commun. **183**, 1845 (2012).
[43] F. Herren and M. Steinhauser, Version 3 of RUNDEC and CRUNDEC, Comput. Phys. Commun. **224**, 333 (2018).
[44] S. A. Larin, T. van Ritbergen, and J. A. M. Vermaseren, The large top quark mass expansion for Higgs boson decays into bottom quarks and into gluons, Phys. Lett. B **362**, 134 (1995).
[45] K. G. Chetyrkin and A. Kwiatkowski, Second order QCD corrections to scalar and pseudoscalar Higgs decays into massive bottom quarks, Nucl. Phys. **B461**, 3 (1996).
[46] W. Bernreuther, L. Chen, and Z.-G. Si, Differential decay rates of CP-even and CP-odd Higgs bosons to top and bottom quarks at NNLO QCD, J. High Energy Phys. 07 (2018) 159.

[47] A. Primo, G. Sasso, G. Somogyi, and F. Tramontano, Exact top Yukawa corrections to Higgs boson decay into bottom quarks, Phys. Rev. D **99**, 054013 (2019).
[48] R. D. Ball *et al.* (NNPDF Collaboration), Parton distributions from high-precision collider data, Eur. Phys. J. C **77**, 663 (2017).
[49] A. Buckley, J. Ferrando, S. Lloyd, K. Nordström, B. Page, M. Rüfenacht, M. Schönherr, and G. Watt, LHAPDF6: Parton density access in the LHC precision era, Eur. Phys. J. C **75**, 132 (2015).
[50] R. Gauld, A. Gehrmann-De Ridder, E. W. N. Glover, A. Huss, and I. Majer, Associated production of a Higgs boson decaying into bottom quarks and a weak vector boson decaying leptonically at NNLO in QCD, J. High Energy Phys. 10 (2019) 002.
[51] W. Bizoń, E. Re, and G. Zanderighi, NNLOPS description of the $H \to b\bar{b}$ decay with MiNLO, J. High Energy Phys. 06 (2020) 006.
[52] J. M. Campbell, S. Höche, H. T. Li, C. T. Preuss, and P. Skands, Towards NNLO + PS matching with sector showers, Phys. Lett. B **836**, 137614 (2023).
[53] S. Alioli, A. Broggio, A. Gavardi, S. Kallweit, M. A. Lim, R. Nagar, D. Napoletano, and L. Rottoli, Resummed predictions for hadronic Higgs boson decays, J. High Energy Phys. 04 (2021) 254.